Mechatronics 49 (2018) 168–176

Contents lists available at ScienceDirect

Mechatronics

journal homepage: www.elsevier.com/locate/mechatronics

Application of hybrid force/position control on parallel machine for mechanical test☆

Julien Le Flohic, Flavien Paccot, Nicolas Bouton, Hélène Chanal*

Université Clermont Auvergne, CNRS, SIGMA Clermont, Institut Pascal, Clermont–Ferrand, F-63000, France

ARTICLE INFO

Keywords:
Parallel machine
Hybrid control
Testing machine
Multi-axial test
Model

ABSTRACT

The quality of mechanical test is strongly linked to the control of boundary conditions and loaded tool path in applied forces or displacement of a tested specimen. In this article, a hybrid force/position control algorithm is adapted to parallel kinematic mechanical test machine with regards to the tested specimen behavior and realized mechanical test. This control algorithm is illustrated on a Nooru–Mohammed test performed on Gough Stewart platform and validated experimentally on a 5 bar parallel mechanism. The principle of the Nooru–Mohamed test consists in submitting a double notched concrete test part to a position slope, inducing a combination of shear and tension loading. The extra degrees of freedom of the parallel machine are used to control boundary conditions.

1. Introduction

Multi-axial tests are used to identify material behavior like concrete [1]. In most cases, damage is localized in areas submitted to multi-axial loading, leading to the failure of the global structure [2]. To explore the specificities of the multi-axial behavior of a material, a solution is to design the testing machine in order to induce multi- axial stress state from a uniaxial actuator. Multi-axial tests are therefore mainly realized with different synchronized structures. However, such machines are not versatile and are designed only for one specific load (tension/compression or tension/torsion for example).

Another solution is to apply directly a multi-axial loading on one specimen using 6 degrees of freedom (DOF) multi-axial testing machine. Thus, the stimulation of a specimen boundary can be achieved by a complete twist (3 translations + 3 rotations), wrench (3 momenta + 3 forces) or a combination of both [3]. This kind of machine can also be used to perform a pure tension test on a specimen with the requirement that non loaded specimen axis are still controlled with a null force.

In this context, the use of 6 DOF parallel kinematic machines can be relevant due to their benefit in term of ability and stiffness compared to serial structure machines [3]. Such parallel kinematic machines (PKMs) have largely been investigated for applications in robotics and machining [4,5]. However, the complexity of associated models and control laws, in addition to a reduced workspace, are their main drawbacks [6,7].

Today, only very few mechanical testing applications have been performed with parallel kinematic machines, and are mainly developed for biomechanical context with large displacements [8–11]. Indeed, extra degrees of freedom are often considerate as disruptive for the specimen load.

Previous works have demonstrated that hexapod architectures are suitable for multi-axial testing of materials through a specific case study, the Nooru–Mohamed (NM) test [2,3] (Fig. 1). Its principle is to load a double edge notched specimen to a combination of shear and tension (or compression) using numerous loading paths [1] and requiring position and/or force control. More clearly, it consists of applying a tool path in one specimen extremity along X and Z axis while no force in Y axis and no torque in X, Y, and Z axis loaded the specimen. According to Nooru–Mohamed, boundary conditions of the tests are difficult to control and since 1992, nobody has been able to perfectly reproduce it with conventional machine. This observation has motivated the development of a test machine based on Gough Stewart platform [2]. First experimentation, during NM test on this Gough Stewart platform, has demonstrated that the instrumentation set up allows a relevant measurement of the displacement field [2]. But this experiment shows an important rigid body motion of the specimen with unwanted force acting on its boundary [11].

Therefore, the aim of this paper is to design an advanced control law for parallel kinematic test machine which ensure to control specimen load and boundary conditions for NM test. In other words, the control algorithm has to control the position of the specimen boundaries on two

☆ This paper was recommended for publication by Associate Editor Lianqing Liu.

* Corresponding author.
E-mail address: helene.chanal@sigma-clermont.fr (H. Chanal).

https://doi.org/10.1016/j.mechatronics.2017.12.006
Received 3 May 2017; Received in revised form 14 November 2017; Accepted 20 December 2017
Available online 05 January 2018
0957-4158/

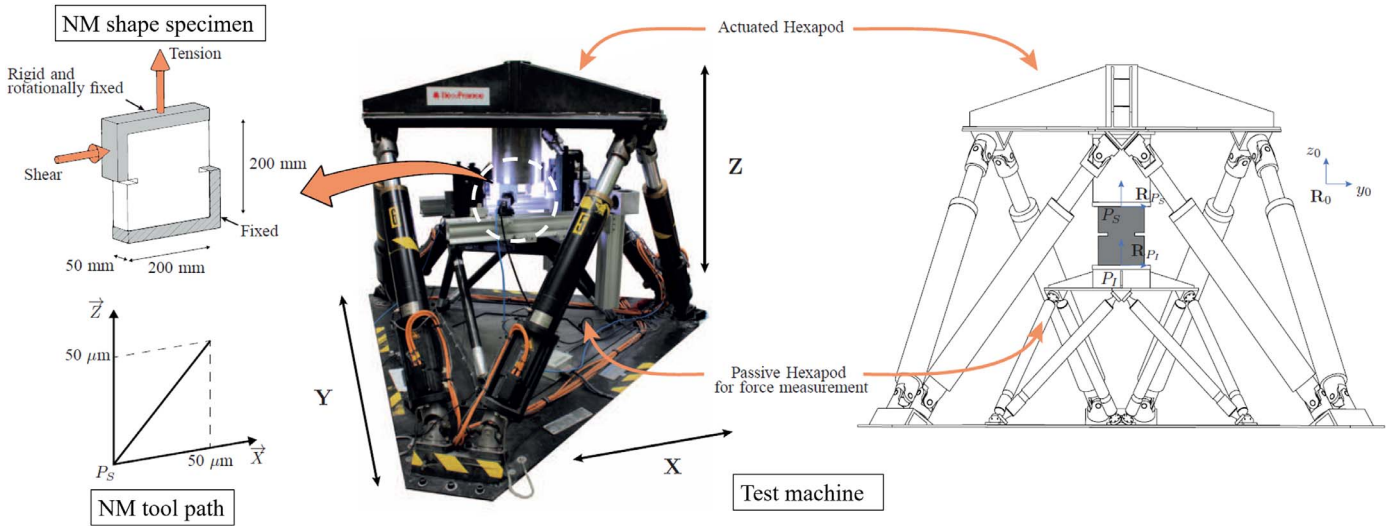

Fig. 1. Principle of Nooru–Mohamed test [1] and test machine.

directions in order to generate the shear and tension load and null forces and torques on the other directions.

To achieve this objective, different methods could be considered and can be classified in two categories: impedance control and hybrid control [12].

Impedance control consists in regulating the mechanical impedance, which is defined as the ratio of force to motion [13]. Therefore, the effort applied by the end-effector on the environment is not directly regulated [14]. It is mainly used for assembling [15], manipulation [16], polishing [17], or more generally for any tasks requiring a position control of a robot which may come into contact with the environment.

The hybrid force control is chosen in particular when the environment is highly deformable, as in a medical context, using flexible environment and tool [18], or when the task requires accurate tracking coupled with high loads, as in a machining context [19,20]. This method is based on the decomposition of the task space into purely motion controlled directions and purely force controlled directions [21,22]. For a 6 DOF parallel manipulator, the n force controlled directions and the 6-n position controlled directions in the Cartesian coordinate system are independently regulated. However, in case of parallel kinematic machine, the movement and force applied by each actuated joint has an influence on the position and the force applied by the mobile platform to the specimen in all Cartesian coordinate system axis.

Then, considering the necessity to control specimen boundaries conditions for a parallel kinematic machine despite the test machine structure deflections for a quasi-static test with complex load trajectory, hybrid force/position control is chosen [11]. Moreover, for NM test, boundaries conditions (null force or torque) and position tool path are defined in the Cartesian space with regard to the specimen.

However, the main limitation of this kind of force control is due to the sensitivity to errors in the implemented dynamic model [10,11]. For NM test, this limitation is overcome assuming that:

- NM test is a quasi-static test. Thus, the test machine static model can be used instead of dynamic model as inertial forces can be neglected. Indeed, the movement of the test machine is very small during the NM test thus just the force and torque applied to the specimen should be controlled.
- NM test generated small movement of actuated joint. Thus, test machine Jacobian matrix can be considered as constant during the test.

The validation of these hypotheses is realized in this article.

In this paper, a hybrid force control law for parallel mechanical test machine is implemented for NM test. This paper presents a method to define a hybrid force control law and its tuning method from the mechanical behavior modeling of the tested specimen and the machine with regard to the test requirement. The experimental validation of the proposed control law is realized on a 5 bar parallel robot as the implementation on the final hexapod requires other important developments.

The proposed control law was firstly introduced in references [23] and [24]. This paper particular contribution is the discussion of this control law and experimental validation on 5 bar parallel mechanism. Thus, this last study ensures to validate the real application of the control scheme and the possible generalization of the proposed method.

The paper is organized as follows. Section 2 presents the hexapod test machine and the model associated. Based on this formalism, Section 3 describes the control scheme implemented. Section 4 presents a first result discussion based on simulations realized on a Simulink®/Adams™ environment. Finally, the defined control law is applied and validated on a 5 bar parallel mechanism.

2. Presentation of test machine

A first experimentation of NM test with a hexapod mechanical test machine has been performed in reference [8]. It revealed that an advanced control law is needed to use extra DOF to have an accurate control of boundary conditions. This test shown that displacement at failure is negligible in comparison to the specimen dimension (0.01%).

During this test, position of the upper limit of the specimen and the load on the specimen are measured with a position sensors and force/torque sensors (Fig. 1).

In a first time, the hexapod test machine and its instrumentation is introduced before the definition of associated model.

2.1. Hexapod test machine

The hexapod test machine is composed of an actuated machine (6 DOF Bosch–Rexroth hexapod with ballscrew electrically actuated cylinder) and a passive hexapod for force measurement. The specimen is placed between this two hexapodes (Figs. 1 and 2). The force and torque measurement is realized with an uncertainty of 80 N and 20 N.m [25]. This instrumentation enables a resolution of 0.2 μm with a 20 Hz frame rate.

The displacement between the two specimen extremities is achieved

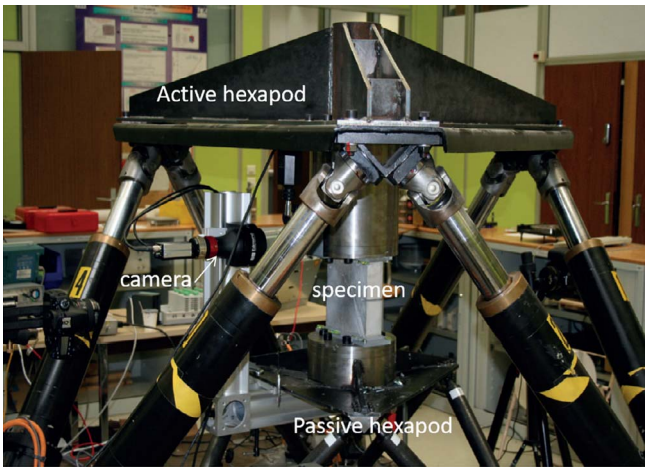

Fig. 2. Hexapod test machine.

with a set of cameras coupled with an integrated digital image correlation technique [26]. Cameras are fixed to the bottom of the specimen and measure the displacement of the top of the specimen. Then, displacements due to the flexibility of the structure are not taken into account in the measurement of the specimen deformation and regulation can be directly realized with regard to specimen load and surfaces displacement. This is the main benefit of this hexapod test machine compared to other one like in Wang's work [11]. Indeed, an implementation of hexapod structure flexible model on the control law is not necessary.

Mechanical features of actuated hexapod machine are listed in Table 1 and show that it is adapted to mechanical tests on concrete.

2.2. Modeling of hexapod test machine

The parameters of hexapod test machine are given in Fig. 3. $\mathbf{X} = [x, y, z, \psi, \theta, \phi]^T$ is a 6-components vector which represents the pose of the upper specimen surface with regard to the lower specimen surface. x, y and z are the components of the origin P_S linked to the end effector with regard to the frame $\mathbf{R}_{PI}$ linked to the base (Fig. 3). ψ, θ and ϕ are the Euler angles which represents the orientation of frame $\mathbf{R}_{P_S}$ with regard to $\mathbf{R}_{PI}$. $\mathbf{q} = [q_1, q_2, q_3, q_4, q_5, q_6]^T$ represents the length of each actuated joint. Further details can be found in reference [2].

As this machine is used for the NM test, i.e. for generating a quasi-static load with a very low speed (15 µm/min), dynamic forces can be neglected with regard to static ones. To link the force applied by the end effector to the actuated joint torques/forces, the static model is used.

The static model of a parallel machine is the mathematical relation which links the actuated joint torques/forces with the force applied by the end effector [1]. In case of parallel kinematic machine, principle of virtual works is classically applied [27,28]:

$$\mathbf{f} = \mathbf{J}^{\mathrm{T}}\Gamma \tag{1}$$

where $\mathbf{\Gamma}$ is the torque/force vector applied by the end effector. The vector $\mathbf{f}$ represents the actuated joint torque/force. $\mathbf{J}^{\mathrm{T}}$ is the geometric transposed Jacobian matrix. The Jacobian matrix is defined as:

Table 1
Loads capacity of hexapod in neutral position.

	Axe X	Axe Y	Axe Z
Force	58 kN	54 kN	126 kN
Torque	46 kNm	41 kNm	71 kNm
Translation resolution	3.95 µm	0.54 µm	0.19 µm

$$\dot{\mathbf{q}} = \mathbf{J}^{-1}\dot{\mathbf{X}} \tag{2}$$

where $\dot{\mathbf{q}}$ is the actuated joint velocity and $\dot{\mathbf{X}}$ the end effector velocity in Cartesian coordinate system.

$\mathbf{J}^{-1}$ is computed from the inverse kinematic model (IKM):

$$\mathbf{J}^{-1} = \frac{\partial \mathrm{IKM}(\mathbf{X})}{\partial \mathbf{X}} \text{ with } \mathbf{q} = \mathrm{IKM}(\mathbf{X}) \tag{3}$$

IKM of the Gough Stewart platform is well known and publish several times in literature [4].

As NM test is a quasi-static test, only small displacement of the end-effector is induced (less than 0.002% of the total displacement at the failure, at about 17000 N). Thus, we can assume that $\mathbf{J}$ can be considered as constant during this mechanical test. This assumption allows simplifying the hybrid force/position control law implementation.

3. Hybrid force/position control scheme

Hybrid force/position control ensure to control axes on position, and axes on force in the same time [22]. The selection is made by a matrix $\mathbf{S}$ which indicate how the axis is controlled [14]:

$$\mathbf{S} = \begin{bmatrix} s_1 & 0 & 0 & 0 & 0 & 0 \\ 0 & s_2 & 0 & 0 & 0 & 0 \\ 0 & 0 & s_3 & 0 & 0 & 0 \\ 0 & 0 & 0 & s_4 & 0 & 0 \\ 0 & 0 & 0 & 0 & s_5 & 0 \\ 0 & 0 & 0 & 0 & 0 & s_6 \end{bmatrix} \tag{4}$$

With

- $s_i = 1$ if axis i is position controlled
- $s_i = 0$ if axis i is force controlled

Fig. 4 presents the control scheme with:

- $\mathbf{X}^{\mathrm{d}}$ and $\mathbf{\Gamma}^{\mathrm{d}}$ the desired position and force/torque
- $\mathbf{e}_{\mathrm{X}} = \mathbf{X}^{\mathrm{d}} - \mathbf{X}$ and $\mathbf{e}_{\Gamma} = \Gamma^{\mathrm{d}} - \Gamma$, the position and force error
- PCL the position control law (output: $\mathbf{\Gamma}_{\mathrm{PCL}}$) and FCL the force control law (output: $\mathbf{\Gamma}_{\mathrm{FCL}}$)

Controls from position and force loop are then mixed together to form a global control vector $\mathbf{G}$.

The application of a hybrid force control scheme requires orthogonality between axis controlled in position and axis controlled in force. This fact can be validated by computing the reciprocal product of Ball [29]:

$$\mathbf{w}.\ \mathbf{T} = [\mathbf{f}; \mathbf{m}].\ [\mathbf{V}; \Omega] = \mathbf{f}.\ \mathbf{V} + \mathbf{m}.\ \Omega = 0 \tag{5}$$

Where $\mathbf{f}$ is the vector of controlled forces, $\mathbf{m}$ the vector of controlled torques, $\mathbf{V}$ the vector of controlled linear displacements, and $\mathbf{\Omega}$ the vector of controlled angular displacements. In the case of NM test, the control scheme has to guarantee that no force is applied in Y axis and no torque in X, Y, and Z axis, thus $\mathbf{f} = [0, F_Y, 0]$, and $\mathbf{m} = [M_X, M_Y, M_Z]$. The loading consists of a control tool path along X and Z axis, thus $\mathbf{V} = [V_X, 0, V_Z]$ and $\Omega = [0, 0, 0]$. Thus, the application of Eq. (4) ensure to validate the applicability of hybrid force control in the case of NM test.

As the regulation is directly realized with regard to specimen behavior, a mechanical model of the specimen behavior during NM test is used to design and tune the control law. This model is obtained from a classical concrete model by considering the Young's modulus and Poisson's ratio of the material [30]:

$$\Gamma_{Mod-mat} = \mathbf{R}\mathbf{X} + \mathbf{C}\dot{\mathbf{X}} \tag{6}$$

with $\mathbf{R}$ the stiffness vector and $\mathbf{C}$ the damping vector of the studied material.

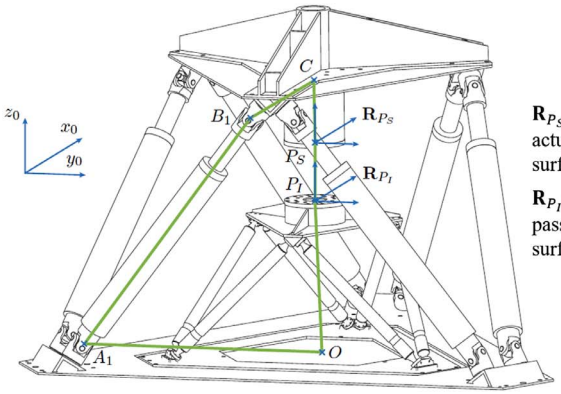

Fig. 3. Hexapod test machine parameters.

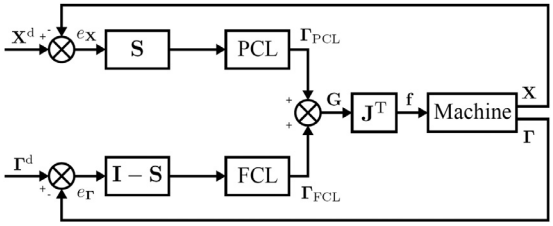

Fig. 4. Hybrid force/position control scheme.

The two position and force control law are detailed in the reminder of this paragraph.

3.1. Position control law (PCL)

The design of PCL is realized to control the variation of the position error $\mathbf{e}_X$ with regard to time. A proportional/integral corrector is used to cancel the ramp tracking error. The first control law ($\mathbf{\Gamma}_{PCL}$) is design from:

$$\dot{\mathbf{e}}_X = \dot{\mathbf{X}}^d - \dot{\mathbf{X}} = -\mathbf{K}_P\mathbf{e}_X - \mathbf{K}_{Ip}\int \mathbf{e}_X \tag{7}$$

where $\mathbf{K}_P$ is the proportional gain vector, and $\mathbf{K}_{Ip}$ is the integral gain vector. To impose time characteristics of the second order decrease of the error e, the tuning is:

$$K_{Pi} = 2\xi_i\omega_{0i} \text{ and } K_{Ipi} = {\omega_{0i}}^2 \tag{8}$$

The damping ξ_i is used to regulate the transitional regime and avoid oscillations. It should be greater than or equal to 1 to obtain a soft behavior during shocks caused by specimen small cracks. ω_{0i} is tuned considering the desired five percent settling time $tr_{5\%i}$, but should be small enough to avoid disruptive shocks due to control law behavior. From Eqs. (6) and (7):

$$\dot{\mathbf{X}}^d - \mathbf{C}^{-1}(\Gamma_{Mod-mat} - \mathbf{RX}) = -\mathbf{K}_P\mathbf{e}_X - \mathbf{K}_{Ip}\int \mathbf{e}_X \tag{9}$$

In the case of NM test, $\Gamma_{Mod-mat}$ is the control vector which ensure to follow the desired tool path along X and Z axis, thus $\Gamma_{Mod-mat} = \Gamma_{PCL}$. Finally, $\mathbf{\Gamma}_{PCL}$ can be computed from:

$$\Gamma_{PCL} = \mathbf{K}_P\mathbf{C}\mathbf{e}_X + \mathbf{RX} + \mathbf{C}\dot{\mathbf{X}}^d + \mathbf{K}_{Ip}\mathbf{C}\int \mathbf{e}_X \tag{10}$$

Thus, perturbations can occur from modeling errors of material behavior. Thus, a first identification step is necessary to guarantee the accuracy of realized mechanical test.

3.1.1. Force control law (FCL)

An exponential decrease of the first-order error is chosen (control forces values are fixed). An integral action is introduced in order to obtain error decrease to 0.

The force control law ($\mathbf{\Gamma}_{FCL}$) is based on the force error $\mathbf{e}_\Gamma$ expression:

$$\mathbf{e}_\Gamma = \Gamma^d - \Gamma = -\mathbf{K}_{If}\int \mathbf{e}_\Gamma \tag{11}$$

Thereby $\mathbf{K}_{If}$, the integral gain vector, allows to impose the error first order decrease to 0 with:

$$\frac{3}{K_{If_i}} = tr_{5\%i} \tag{12}$$

Each K_{Ifi} is tunable for each axis i.

In the case of force control, $\mathbf{\Gamma}$ is the control vector which should to be null for NM test, thus $\Gamma = \Gamma_{PCL}$. Finally, $\mathbf{\Gamma}_{FCL}$ can be computed from:

$$\Gamma_{FCL} = \Gamma^d + \mathbf{K}_{If}\int \mathbf{e}_\Gamma \tag{13}$$

3.1.2. Global control law

Due to the shape of the matrix $\mathbf{S}$ (see Eq. (4)), $\mathbf{\Gamma}_{PCL}\mathbf{S}$ and $\Gamma_{FCL}(\mathbf{I} - \mathbf{S})$ are orthogonal and are then added to form vector $\mathbf{G} = \mathbf{S}\Gamma_{PCL} + (\mathbf{I} - \mathbf{S})\Gamma_{FCL}$. The 6 axis of the Cartesian coordinate system are controlled. Finally, forces applied by the 6 actuated joint of hexapod test machine are:

$$\mathbf{f} = \mathbf{J}^T\mathbf{G} \tag{14}$$

3.2. Control law interpretation

The control scheme is designed from the specificity of NM test and testing material characteristics. Thus, $\mathbf{\Gamma}_{PCL}$ is defined from a tested material behavior model with a second order to regulate a position slope. $\mathbf{\Gamma}_{FCL}$ allows regulating a fixed load, it is naturally a first order with a force anticipation term and an integral term.

This strategy is thus consistent with the material behavior and with the desired trajectory as long as the specimen is not broken. When the workpiece fails, the test is over and the actuators are immediately stopped [2]. Note that the parallel robot gravity is directly compensated in the Bosch controller.

First result from simulation environment is introduced in the next section.

4. Simulated results

To validate the developed hybrid force/position control law, a model of hexapod test machine and specimen behavior is defined in a multi-body dynamic software Adams™. This model is coupled with Simulink® to simulate the control law behavior. The global scheme is presented on Fig. 5.

The developed hybrid force/position (HFP) controller is compared with the initial regulated strategy implemented in hexapod test machine [2]. This first controller consists in regulated each axis with a proportional-integral (PI) regulation.

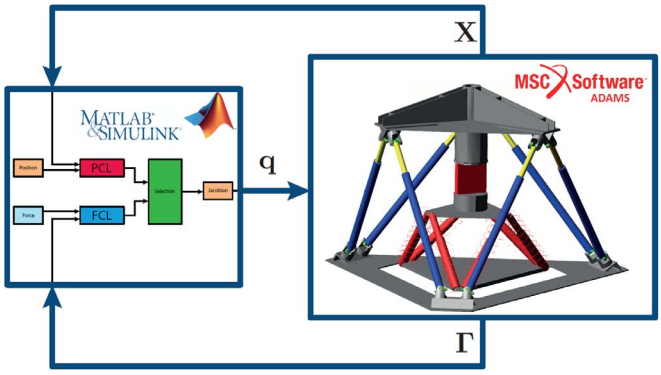

Fig. 5. Simulation environment.

The real sensors measurement behaviors are simulated by generating a sampled and noised signal with regard to the real resolution and frame rate of the cameras. To take into account the specimen material model uncertainties, an error of 10% is applied to the matrix **R** and **C**.

An offset of 1 µm is introduced to the position trajectory to take into account the displacement induced by the breaks opening at the beginning of the experiment. A specimen preload on axis Y is simulated to model the load applied by the drying of the glue used to fix the specimen on the machine. Moreover, a step effort is applied to the hexapod at $t = 2\,\text{s}$ ($F_X = 300\,\text{N}$, $F_Y = 200\,\text{N}$ and $F_Z = 400\,\text{N}$) to simulate a partial sudden breaks on the specimen due to grit in the concrete or knot in the wood, for example.

This simulation environment ensures to validate the benefit brings by HFP for mechanical test on parallel kinematic machine.

4.1. Nooru–Mohamed test simulation

A $X-Z$ slope trajectory is imposed with a 15 µm/min velocity. Fig. 6 shows that both controllers allow to correctly follow the trajectory with almost identical error behavior. For HPF control law, $tr_{5\%i}$ is tune in order to obtain a behavior consistent with the quasi-static hypothesis, and soft enough to avoid shocks: $tr_{5\%} = 300\ ms$ for force control law and $tr_{5\%} = 1\ s$ for position control law. PI control law is tuned with $tr_{5\%} = 1\ s$.

Fig. 7 shows the main benefit of HFP. Indeed, only HFP strategy ensures to compensate the Y direction preload and a partial sudden crack. The hybrid strategy uses extra DOF to generate a rigid body motion which guarantees the boundaries conditions of unsolicited axis.

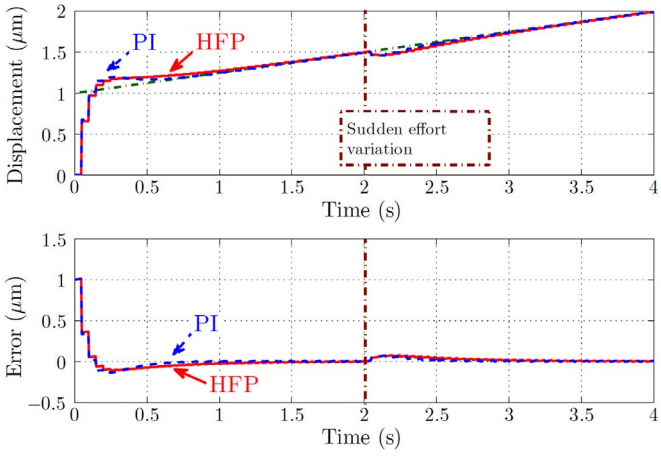

Fig. 6. Trajectory on axis X (Top) and error e_x (Bottom) for position loop. (Graph for Z direction are about the same).

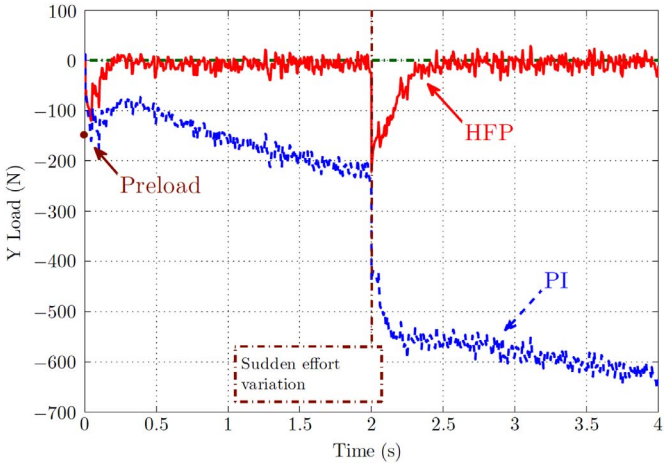

Fig. 7. Force on the unsolicited axis Y.

Finally with HFP strategy, the concrete specimen is only loaded on X and Z directions, as desired.

4.2. Sensibility of HFP

In order to determine the control sensibility to perturbations during NM test, different kinds of errors are identified and isolated. Results are summarized in Table 2.

4.2.1. Error in the kinematic model

First part of Table 2 presents the time answer characteristics of HFP controller with a percentage of error in the kinematic parameters.

It shows that the Jacobian is not sensitive to geometric errors as overshoot on axes X and Z (measured on the position error results) is nearly the same even with important errors. This behavior is due to the small displacement induced by NM test and it validates the hypothesis of quasi-static test.

4.2.2. Error in the specimen model

In the second part of Table 2, performance of the HFP controller are presented for defect on the specimen model parameters used for the

Table 2
Robustness analysis of proposed solution (HFP).

Error in the kinematic model (see 4.3.1)			
Error	Overshoot X (µm)	Overshoot Z (µm)	Overshoot Y (N)
0%	10.95%	11.04%	0
1%	10.94%	11.04%	0
10%	11.05%	11.00%	0
50%	10.10%	11.8%	0
Error in the specimen model (see 4.3.2)			
Error	Overshoot X (µm)	Overshoot Z (µm)	Overshoot Y (N)
0%	10.95%	11.04%	0
1%	10.92%	11.00%	0
10%	10.54%	10.62%	0
50%	14.35%	14.61%	0
Partial sudden breaks (see 4.3.3)			
Effort	Step X (µm)	Step Z (µm)	Settling time Y (s)
100 N	0.0211	0.0139	0.10
300 N	0.0578	0.0447	0.20
500 N	0.0946	0.0756	0.25

force and position control law. The impacts become important just for large error. Indeed, there is a link between the specimen model and the tuning of the control laws. It is still negligible up to 20%, which could be considered as acceptable.

4.2.3. Partial sudden break

In order to observe the impact of partial sudden break that can occur during a real test on concrete, the third part of Table 2 presents the displacement for axis controlled in position or settling time for axis controlled in force generated by a partial sudden break during the test.

Previous NM test referred in [2] showed that this shocks are order of 200 N. Results illustrate one of main benefit of HFP which is that even with a 500 N shock, controller is able to adapt the trajectory in a short time to respect boundaries conditions with an induced displacement for position controlled axis less than 0.1 μm.

4.3. Summary of simulation results

This section presents the design of a hybrid force/position controller adapted to a hexapod test machine, to the behavior of specimen material and to the NM test specificities. Simulations show that this strategy is more relevant than the previous controller (PI axis by axis), indeed, unwanted load are avoided and boundary conditions are controlled.

As the hexapod test machine is not in our laboratory workshop and in order to validate in a first way the proposed strategy and the adaptation to other loading machine, we applied this methodology in a 5 bar parallel mechanism.

5. Experimental validation with a 5 bar parallel mechanism

This section illustrates the proposed HFP command strategy on a 5 bar parallel mechanism which provides only movement in a plane. The mechanical test is realized in two directions: one direction controlled in position, the other in force. A preloaded spring replaces the specimen part.

In a first time, the used 5 bar parallel mechanism is introduced. Then, the geometrical and static models are presented. Finally, the results are analyzed.

5.1. 5 bar mechanism

A 5 bar mechanism is a planar parallel robot which is composed with 2 legs linked to a revolute joint positioned at point *C*. Each leg is composed of an actuator located at the revolute joint positioned at point A_i and a passive joint at point B_i (Fig. 8). This mechanism is usually used to study singularities [31]. However, in our case the test is positioned far from the singularity.

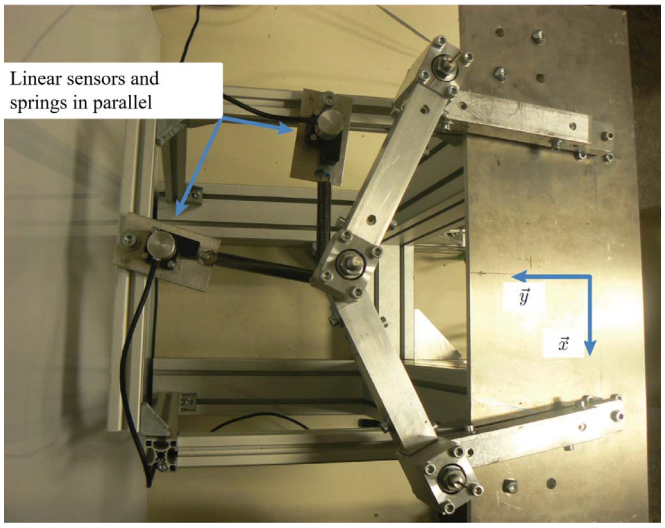

Fig. 9. Configuration of the used 5 bar mechanism for mechanical test.

The used 5 bar mechanism is realized with aluminum parts and joints made with roller bearings. The mechanism is actuated using 2 PARVEX brushless servo motors and two 1/15 gear boxes. The servo motors are controlled using an Adept control architecture working with a C++ software developed by Adept France, CIDE, which ensures to develop a computed torque control law.

In order to realize mechanical test, 2 linear sensors (Micro-Epsilon WPS-750-MK30-E) are added on the 5 bar mechanism. These sensors have a resolution of 0.038 mm (Fig. 9). Two springs are positioned in parallel of these sensors: one is used to measure force applied to the end-effector in the controlled force direction, the other is used to simulate the presence of a specimen in the controlled position direction.

In order to apply the methodology, geometrical and statics modeling are provided.

5.2. Modeling of 5 bar mechanism

5 bar geometrical modeling is based on the geometrical closed loop which define the geometrical behavior of 5 bar mechanism.

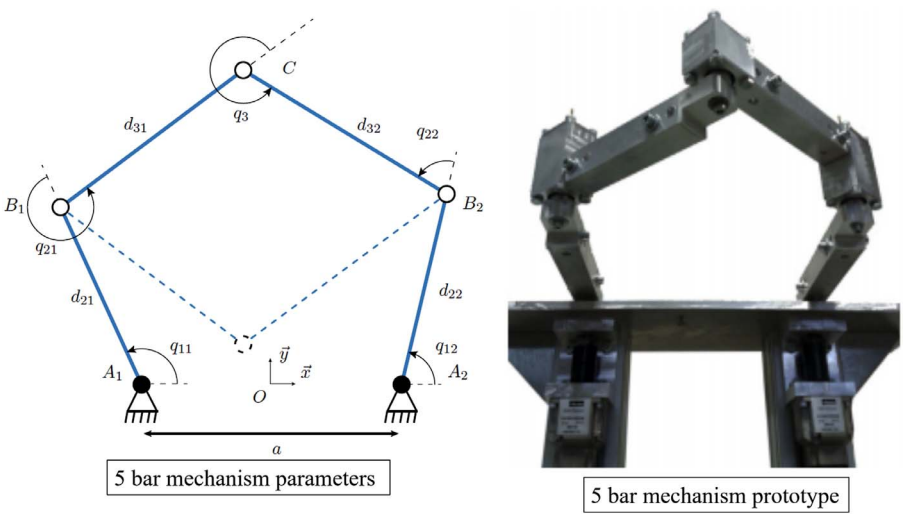

Fig. 8. 5 bar mechanism used for this study [31].

Table 3
5 bar mechanism geometrical parameters [31].

Parameters	a	d_{21}	d_{22}	d_{31}	d_{32}
Identified values	0.2822 m	0.2130 m	0.2130 m	0.1888 m	0.1878 m

5.2.1. Geometrical modeling

In order to compute geometrical model, the following geometrical equations are considered:

$$\begin{cases} x - x_{A_i} - d_{2i}\cos q_{1i} - d_{3i}\cos(q_{1i} + q_{2i}) = 0 \\ y - y_{A_i} - d_{2i}\sin q_{1i} - d_{3i}\sin(q_{1i} + q_{2i}) = 0 \end{cases} \quad (15)$$

With x and y the coordinate of point C, x_{A_i} and y_{A_i} the coordinate of point A_i and other parameters is described in Fig. 8.

Moreover, articular coordinates satisfy:

$$\pi - q_{11} - q_{21} - q_{31} + q_{12} + q_{22} = 0 \quad (16)$$

Points B_i coordinates (x_{B_i}, y_{B_i}) satisfy:

$$\begin{cases} x_{B_i} = x_{A_i} + d_{2i}\cos q_{1i} \\ y_{B_i} = y_{A_i} + d_{2i}\sin q_{1i} \\ d_{3i}^2 = (x - x_{B_i})^2 + (y - y_{B_i})^2 \end{cases} \quad (17)$$

Thus, the direct geometrical model is computed by using Eqs. (15), (16) and (17).

The value of geometrical parameters of the used 5 bar mechanism is presented in Table 3 according to Pagis' identification process [31].

5.2.2. Statics modeling

As Nooru–Mohamed test is a realized with a low speed, we can assume that dynamic effects have no influence on the effector motion. Thus, only the statics modeling is used in the control scheme. The computation of Jacobian matrix **J** ensures to compute the motor torques with regard to force applied on the end-effector.

J is computed with a derivation of Eq. (17):

$$\mathbf{J} = \mathbf{A}^{-1}\mathbf{B} \quad (18)$$

with $\mathbf{A} = \begin{bmatrix} 2(x + \frac{a}{2} - d_{21}\cos q_1) & 2(y - d_{21}\sin q_1) \\ 2(x - \frac{a}{2} - d_{22}\cos q_2) & 2(y - d_{22}\sin q_2) \end{bmatrix}$ and $\mathbf{B} = \begin{bmatrix} -2d_{21}\sin q_1\left(x + \frac{a}{2}\right) + 2yd_{21}\cos q_1 & 0 \\ 0 & -2d_{22}\sin q_2\left(x - \frac{a}{2}\right) + 2yd_{22}\cos q_2 \end{bmatrix}$.

To develop and tune the control scheme, after the identification of geometrical parameters, the added springs behavior has to be modeled and identified (Eq. (6) for a real concrete specimen).

5.2.3. Identification of spring behavior

As the test is quasi-static, we consider that spring behavior is represented by its preload P_r, its stiffness R and its viscosity C. The force applied by the spring can then be computed with Eq. (6) by adding a preload term. The stiffness and preload parameters are identified with a traction machine. The relation between force applied to the spring and its displacement is given in Fig. 10.

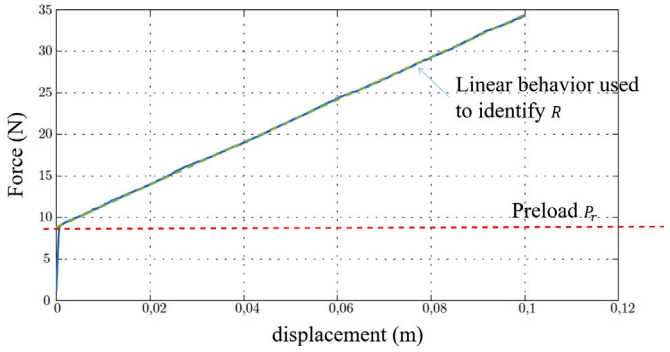

Fig. 10. Data to identify stiffness and preload spring identification.

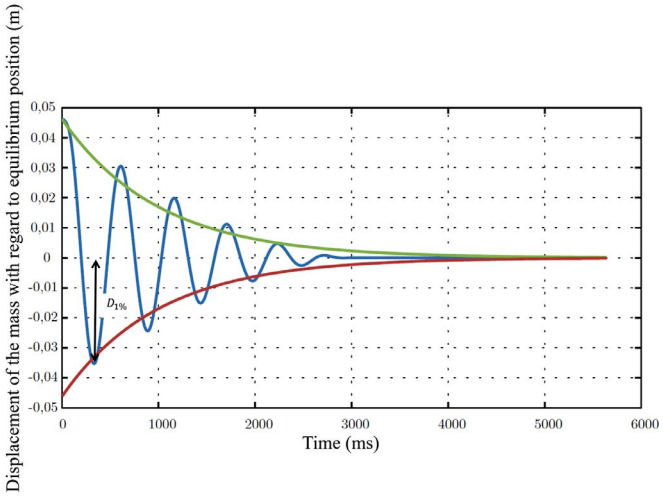

Fig. 11. Viscosity identification.

The viscosity C is identified by exiting the spring with a mass M (Fig. 11). The first overshoot $D_{1\%}$ allows to identify the damping ratio ξ and then the viscosity:

$$D_{1\%} = e^{-\pi\frac{\xi}{\sqrt{1-\xi^2}}} \quad (19)$$

$$C = \frac{2R\xi}{\sqrt{R/M}} \quad (20)$$

Finally, parameters of the 2 springs are given in Table 4.

According to Eq. (8) and (12) with a control scheme damping $\xi = 1$ and $\omega_0 = \frac{5}{tr_{5\%}}$, HFP gains can be expressed as:

$$\begin{cases} K_P = 10/tr_{5\%} \\ K_{Ip} = 25/tr_{5\%}^2 \\ K_{If} = 3/tr_{5\%} \end{cases} \quad (21)$$

Initial gains values are given in Table 5. However, with these settings, a too high overshoot appears due to the presence of mechanical joint slacks. Thus, gain K_{Ip} is experimentally tuned to 20000 s^{-1}.

5.3. Results

In order to validate the proposed HFP control scheme for mechanical test, axis X is controlled in position and axis Y is controlled in force (Fig. 9). The control tool path in position is a ramp set point with a speed of 50 mm/min while the set point in force is constant and equal to 22 N.

At $t = 16$ s, a disruptive exterior load is applied to the end-effector and the stiffness in axis Y is modified. In practice, we modify the stiffness of the specimen by removing a little spring connected in parallel of one of the identified spring. The generated shock is near 1 N. Figs. 12 and 13 presented the measured curve of the position variation along axis X and the estimated curve of the force variation along axis Y.

Thus, despite the initial preload and disruptive exterior load in the middle of the experimentation, the force value axis y remains closed to desired force value. In case of PI control law, a deviation is observed during our simulation with a Gough Stewart platform (Fig. 7). Thus, HFP scheme is validated for mechanical test. Indeed, the specimen follows the attempted toolpath in axis X despite the perturbation generated by the stiffness modification in axis Y. Due to this stiffness

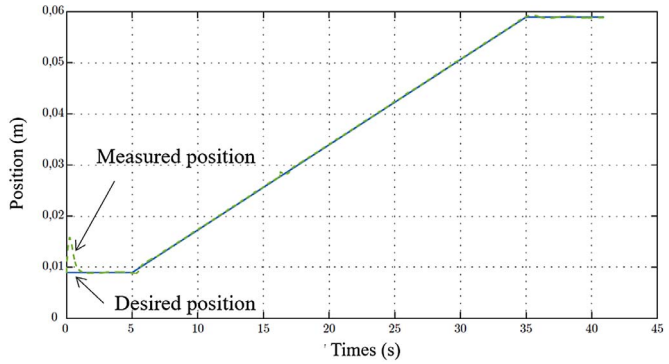

Fig. 12. Measure of the position along axis ***X*** during the HFP test in 5 bar mechanism.

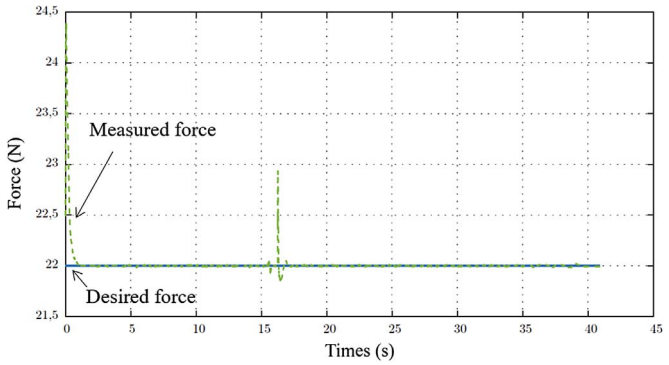

Fig. 13. Estimation of the force along axis ***Y*** during the HFP test in 5 bar mechanism.

Table 4
Identified parameters for modeling spring behavior.

	Stiffness R	Preload P_r	Viscosity C
Spring 1	255.74 N.m	8.83 N	3.81
Spring 2	242.48 N.m	10.48 N	4.13

Table 5
HFP gains values.

Gains	$tr_{5\%}$	K_P	K_{Ip}	K_{If}
Initial value	0.03 s	333 s^{-1}	27778 s^{-2}	100 s^{-1}
Final value	0.03 s	333 s^{-1}	20000 s^{-2}	100 s^{-1}

modification, the robot has applied a rigid body motion along axis Y in order to keep an applied force of 22 N without modifying the tool path along axis X. The same behavior is observed during the simulation on the hexapod test machine.

Moreover, even if the modeling and identification of 5 bar mechanism behavior is not accurate as joint friction and clearances are not considered, the boundaries of the specimen follow the expected tool path. This observation is consistent with the conclusion of paragraph 4.2.1 on the sensibility to error in kinematic model and the hypothesis about a quasi-static loaded of test machine.

This experimentation ensures to validate that HFP control law which is relevant for mechanical test with parallel machine. Despite the uncertainty of parameters identification of robot stiffness and geometrical parameters and despite the disruptive load which is due to the material heterogeneity or machine structure stiffness, this control law allows using all the robot axis to control boundary condition of the specimen. Thus, this work open the way of new multi-axis mechanical tests.

6. Conclusion

Contribution of this paper is to propose, in a context of mechanical test, a complete strategy which allows to perfectly control the test course based on mechanical modeling of the test machine and tested specimen behavior.

Introducing mechanical notions in the control process allows having a behavior directly linked to the structure, the specimen and mechanical test specificity. Second point is that assumptions in relation with the task specificities are made to make technically feasible the realization of this advanced controller.

The strategy developed is adaptable and it is easily to achieve other kind of loading tests. However, it is necessary to check the viability of the assumptions made, particularly with highly deformable specimen as elastomer.

Acknowledgment

This work has been sponsored by the French government research through a ministerial doctoral grant.

This work was carried out within the Manufacturing 21 working group, which comprises 18 French research laboratories. The topics approached are: modeling of the manufacturing process, virtual machining, emergence of new manufacturing methods.

References

[1] Nooru-Mohamed MB. Mixed mode fracture of concrete: an experimental approach. Doctoral thesis Delft University; 1992.
[2] Nierenberger M, Poncelet M, Pattofatto S, Hamouche A, Raka B, Virely JM. Multiaxial testing of materials using a Stewart platform: case study of the Nooru-Mohamed test. Exp Tech 2012. http://dx.doi.org/10.1111/j.1747-1567.2012.00807.x.
[3] Le Flohic J, Parpoil V, Bouissou S, Poncelet M, Leclerc H. A 3D displacement control by digital image correlation for the multiaxial testing of materials with a Stewart platform. Exp Mech 2014;54(5):817–28. http://dx.doi.org/10.1007/s11340-013-9837-z.
[4] Merlet JP. Parallel robots. 2nd edition Dordrecht: Springer; 2006.
[5] Chanal H, Duc E, Ray P. A study of the impact of machine tool structure on machining processes. Int J Mach Tools Manuf 2006;46(2):98–106.
[6] Paccot F, Andreff N, Martinet P. A review on dynamic control of parallel kinematic machine: theory and experiments. Int J Rob Res 2009;28(3):395–416.
[7] Merlet JP. Still a long way to go on the road for parallel mechanisms. Montreal: ASME 27th Biennial Mechanisms and Robotics Conf.; 2002.
[8] Stokes IA, Gardner-Morse M, Churchill D, Laible JP. Measurement of a spinal motion segment stiffness matrix. J Biomech 2002;35:517–21.
[9] Michopoulos JG, Hermanson JC, Furukawa T. Towards the robotic characterization of the constitutive response of composite materials. Compos Struct 2008;86:154–64.
[10] Goertzen J, Kawchuk N. A novel application of velocity-based force control for use in robotic biomechanical testing. J Biomech 2009;42:366–9.
[11] Wang D, Fan R, Chen W. Simulation research on adaptive control of a six-degree-of-freedom material-testing machine. Int J Adv Robot Syst 2014;11(1):1–13. http://dx.doi.org/10.5772/57463.
[12] De Schutter J, Bruyninckx H, Zhu WH, Spong MW. Force control: a bird's eye view. IEEE CSS/RAS International Workshop on Control Problems in Robotics and Automation: Future Directions. 1997.
[13] Hogan N. Impedance control: an approach to manipulation. Trans ASME J Dyn Syst Meas Control 1985;107:1–24.
[14] Khalil W, Dombre E. Modeling, identification & control of robots. HERMES Penton Science; 2002.
[15] Lopes A, Almeida F. A force-impedance controlled industrial robot using an active robotic auxiliary device. Robot Comput Integr Manuf 2008;24:299–309.
[16] Park JH, Cho HC. Impedance control with varying stiffness for parallel-link manipulators. Proceedings of the American Control Conference. 1998.
[17] Nagata F, Hase T, Haga Z, Omoto M, Watanabe K. CAD/CAM-based position/force controller for a mold polishing robot. Mechatronics 2007;17(4–5):207–16. http://dx.doi.org/10.1016/j.mechatronics.2007.01.003.
[18] Madani M, Moallem M. Hybrid position/force control of a flexible parallel

manipulator. J Franklin Inst 2011;348:999–1012.
[19] Zhao X, Pan Y. Draft: force-position hybrid control of a new parallel hexapod robot for drilling holes on fuselage surface. ASME 2013 International Design Engineering Technical Conf. & Computers and informations in Engineering Conf. 2013.
[20] Satya SM, Ferreira PM, Spong MW. Hybrid control of a planar 3 DOF parallel manipulator for machining operations. Trans NAMRI/SME 1995;23:273–80.
[21] Raibert MH, Craig JJ. Hybrid positon/force control of manipulators. Trans ASME J Dyn Syst Meas Control 1981;103:126–33.
[22] Raibert MJ, Craig JJ. Hybrid position/force control of manipulators. ASME J Dyn Syst Meas Contr 1981;103:126–33.
[23] Le Flohic J, Paccot F, Bouton N, Chanal H. Enhancing control robustness of a 6 DOF parallel testing machine. European Control Conference (ECC). 2014.
[24] Le Flohic J, Paccot F, Bouton N, Chanal H. A hybrid force/position control for 6 DOF parallel testing machine. Joint Conference on Mechanical, Design Engineering & Advanced Manufacturing. 2014.
[25] Virely JM, Nierenberger M. (ENS Cachan, CNRS) Dispositif de mesure de torseur d'efforts, de structure du type multipode. French Pat Appl 2013:50658. Priority number: FR13Patent pending.
[26] Leclerc H, Périé J-N, Roux S, Hild F. Integrated digital image correlation for the identification of mechanical properties. Lect Notes Comput Sci 2009;5496:161–71.
[27] Sciavicco L, Siciliano B. Modelling and control of robot manipulators. 2nd edition London: Springer; 2001.
[28] Davliakos I, Papadopoulos E. Model-based control of a 6-DOF electrohydraulic Stewart-Gough platform. Mech Mach Theory 2008;43(11):1385–400. http://dx.doi.org/10.1016/j.mechmachtheory.2007.12.002.
[29] Duffy J. The fallacy of modern hybrid control theory that is based on Orthogonal Complements of twist and wrench spaces. J Robot Syst 1990;7(2):139–44.
[30] Bacon C, Pouyet J. Mécanique des solides déformables. Paris: HERMES; 2000.
[31] Pagis G, Bouton N, Briot S, Martinet P. Enlarging parallel robot workspace through Type-2 singularity crossing. Control Eng Pract 2015;39:1–11.

Julien Le Flohic was born in 1987. He received the Ph.D. degree in mechanical engineering from Université Blaise Pascal in 2015. Since 2015, he has been a robotic and control engineer in Delta Dore (Rennes, France).

Flavien Paccot was born in 1981. He received the Ph.D. degree in robotic from Université Blaise Pascal in 2009. Since 2008, he has been a teacher in Université d'Auvergne. His research interests include robotic, control and haptic interface.

Nicolas Bouton was born in 1983. He received the Ph.D. degree in robotic from Université Blaise Pascal in 2009. Since 2010, he has been an assistant professor in SIGMA Clermont. His research interests include robotic and control.

Hélène Chanal was born in 1980. She received the Ph.D. degree in mechanical engineering from Université Blaise Pascal in 2006. Since 2007, she has been an associate professor in SIGMA Clermont. Her research interests include identification and modeling of machine and robot behavior.